Type-I alignment and direct fundamental gap in SiGe based heterostructures

INSTITUTE OF PHYSICS PUBLISHING JOURNAL OF PHYSICS: CONDENSED MATTER

J. Phys.: Condens. Matter **18** (2006) 1021–1031 doi:10.1088/0953-8984/18/3/018

Type-I alignment and direct fundamental gap in SiGe based heterostructures

Michele Virgilio and Giuseppe Grosso

NEST-INFM and Dipartimento di Fisica 'E Fermi', Università di Pisa, Largo Pontecorvo 3, I-56127 Pisa, Italy

E-mail: grosso@df.unipi.it

Received 22 August 2005, in final form 27 October 2005
Published 6 January 2006
Online at stacks.iop.org/JPhysCM/18/1021

Abstract

The electronic properties of strained $Si_{1-x}Ge_x$ alloys epitaxially grown on (001) $Si_{1-y}Ge_y$ relaxed substrates for any x and y Ge concentrations are presented here. Our calculations are based on an $sp^3d^5s^*$ nearest-neighbour tight-binding Hamiltonian and exploit appropriate scaling laws of the Hamiltonian interactions to account for strain effects. Spin–orbit interaction is also included in the Hamiltonian. We first provide the valence and conduction band offsets at the heterointerfaces between $Si_{1-x}Ge_x$ and $Si_{1-y}Ge_y$, as well as the fundamental energy gap for $Si_{1-x}Ge_x$ strained alloys. We are thus able to distinguish the region in the (x, y) plane where robust type-I alignment is achieved. Then this information on band alignment is exploited to propose a heterostructure which is both type I in $\vec{r}$-space and direct in $\vec{k}$-space. With this aim we adopt the decimation–renormalization method for the determination of the electronic properties of the multilayer structure; from the Green's function the energy spectrum and the partial and the total densities of states projected on each layer of the system are obtained. Our conclusion is that by suitable control of alloying, stress, band offsets and folding, truly direct (both in $\vec{r}$- and in $\vec{k}$-space) semiconducting heterostructures based on silicon and germanium can be realized. As an example, the case of pure Ge sandwiched between $Si_{0.25}Ge_{0.75}$ alloys, grown on a $Si_{0.2}Ge_{0.8}$ substrate, is fully discussed.

1. Introduction

In recent years a growing interest has been devoted to the study of coherently strained $Si_{1-x}Ge_x$ alloy layers pseudomorphically deposited on Si(001) substrates. The bonus of bandgap engineering [1] that these systems offer to the integration into Si-based electronics and photonics is the main reason for their technological interest [2–4]. In several applications the electrically active $Si_{1-x}Ge_x$ material is grown not on pure Si but on a relaxed $Si_{1-y}Ge_y$

substrate, or it is sandwiched between regions with defined Si/Ge alloy composition. It is well known [5] that for the unstrained $Si_{1-x}Ge_x$ bulk alloy the electronic band structure is Si-like with sixfold degenerate conduction bands along the Δ-directions if the Ge content is less than 85%, while it assumes Ge-like character with a conduction band minimum at the L point for $x > 85\%$. The bulk alloy lattice constant varies almost linearly with Ge composition as predicted by Vegard's law even if small deviations from it have been detected [6]. Thus the lattice mismatch between $Si_{1-x}Ge_x$ and $Si_{1-y}Ge_y$ depends on the Ge content both in the active layer and in the adjacent alloy. This consequently determines the type of strain along the growth plane in the active material, which is compressive for $x > y$ and tensile for $x < y$. According to the values of x and y concentrations ($0 \leqslant x, y \leqslant 1$) and the growth direction, a variety of different band structures and charge carrier effective masses can be tailored because of the control of chemical composition, of strain conditions and of band offsets. In particular, the problem of defining for a given set of concentrations (x, y) the corresponding band alignment soon emerged as a central item in the theoretical and experimental study of Si/Ge devices (for a review see [1, 2]). Many theoretical and experimental papers have addressed the determination of band alignment, mainly in $Si_{1-x}Ge_x$ alloy epitaxially grown on pure Si in the (001) direction. For such heterostructures general consensus exists on the fact that the alloy active layer constitutes a quantum well for the holes, but the conduction band lineup has appeared more elusive due to the requirement to assign precisely the position of the split Δ_2 and Δ_4 conduction valley energies in the presence of alloying and strain effects. In the end, type-I and type-II band alignment is still a matter of debate for general Si/Ge heterostructures. For the commonly studied (001) heterostructure made by $Si_{1-x}Ge_x$ on pure Si, early theoretical studies based on deformation potential theory [7] and *ab initio* pseudopotential in the local density approximation [8] support type-I lineup for low Ge content. Further calculations based on empirical pseudopotential [9] indicate type-II alignment for all Ge concentrations of the alloy grown on unstrained Si substrate; moreover, type-I alignment is evidenced [9] when a Ge rich active material ($0.75 \leqslant x \leqslant 1$) is grown on a Ge rich alloy substrate ($0.7 \leqslant y \leqslant 1$). The effective mass model for the evaluation of excitonic wavefunctions in $Si_{0.7}Ge_{0.3}$ quantum wells [10] has also proven useful to discriminate between type-I and type-II offsets as proposed by photoluminescence experiments. From the experimental side the question of conduction band lineup at the SiGe/Si heterointerface is still debated. Interpretation of photoluminescence (PL) measurements are made difficult from band-bending, band-filling and binding-energy effects. The analysis of the dependence of the PL energies on intensity [11, 12], on geometry [13] and on hydrostatic [14] and biaxial [15, 16] strain has led authors to claim type I [13–15] and type II [12, 11, 16], alternatively. The first aim of this paper is to provide a full description of valence band and conduction band alignment in a $Si_{1-x}Ge_x$ strained active material epitaxially grown on a relaxed $Si_{1-y}Ge_y$ buffer along the (001) direction, for any Ge concentration $0 \leqslant x, y \leqslant 1$. With respect to previous calculations in the literature [9], we use an $sp^3d^5s^*$ nearest-neighbour tight-binding Hamiltonian [17] which has proven very efficient in the study of Ge quantum wells separated by Si regions of arbitrary width [18]. This Hamiltonian takes into account spin–orbit interactions and can easily consider strain effects by means of suitable scaling laws for the hopping parameters and appropriate elaboration of the tight-binding geometrical phase factors. We confirm a large part of the theoretical results obtained by the authors of [9] by means of the empirical pseudo-potential method; in addition, our results support evidence of inverted type-I alignment (VBO<0, CBO>0) in the (x, y) region where the calculations of [9] seem elusive. After having defined the regions of (x, y) space where type-I or type-II alignments occur, we have addressed the problem of the design of a device with direct gap both in $\vec{r}$-space and in $\vec{k}$-space. For this we have investigated the most general family

of structures constituted by a $Si_{1-x}Ge_x$ active material embedded between two $Si_{1-y}Ge_y$ regions, grown on a relaxed (001)-$Si_{1-z}Ge_z$ substrate. Due to the huge number of atoms in this kind of structure, the decimation–renormalization $\vec{r}$-space method has been adopted to obtain the eigenvalues and eigenfunction of the whole device. The paper is organized as follows: in section 2 we present the theoretical approach used and the results concerning the band structure of the (001) tetragonally distorted $Si_{1-x}Ge_x$ alloy on relaxed $Si_{1-y}Ge_y$ substrate, for any value of the x and y Ge concentrations. In section 3 we exploit the results obtained in section 2 to design a heterostructure which is type I in $\vec{r}$-space and direct in reciprocal space. As an example we report the electronic structure of pure Ge embedded in a thick region of $Si_{0.25}Ge_{0.75}$, grown on a relaxed $Si_{0.2}Ge_{0.8}$ substrate, and we show that it is indeed a genuine type-I and direct-gap material. A comparison is also reported between the optical matrix element of the fundamental transition in this structure and the direct $\Gamma_8^+ \rightarrow \Gamma_6^-$ transition in bulk Ge. Section 4 contains the conclusions.

2. Band lineups of strained $Si_{1-x}Ge_x$ alloys on $Si_{1-y}Ge_y$ substrates

In this section we study the electronic structure of (001)-tetragonally distorted $Si_{1-x}Ge_x$ alloys grown on cubic $Si_{1-y}Ge_y$ alloys. Following [9] we indicate the strained $Si_{1-x}Ge_x$ layers as the *active material* and the relaxed $Si_{1-y}Ge_y$ alloy as the *substrate*. Furthermore, we define as lateral and orthogonal (or growth) the directions parallel and perpendicular to the heterointerface, respectively. For $x > y$ the active layer is biaxially compressed in the lateral direction (for $x < y$ the strain is tensile) due to the matching of its lateral lattice constant $a_\parallel$ with the relaxed substrate lattice constant. As a function of the lattice constant a_0(Ge) and a_0(Si) for pure Ge and pure Si, respectively, the substrate bulk alloy lattice constant is given by [9, 19]

$$a_0(y) = a_0(\mathrm{Si}) + 0.200\,326\; y\,(1-y) \;+\; [a_0(\mathrm{Ge}) - a_0(\mathrm{Si})]\; y^2 \text{ Å}. \tag{1}$$

The orthogonal lattice constant in the active material is well reproduced by elasticity theory [4] and is given by

$$a_\perp(x) = a_0(x)\left(1 - 2\frac{c_{12}(x)}{c_{11}(x)}\frac{a_\parallel(x) - a_0(x)}{a_0(x)}\right), \tag{2}$$

where $a_0(x)$ is the lattice constant of the relaxed active layer and $c_{11}(x)$ and $c_{12}(x)$ are the elastic constants of the alloy obtained interpolating linearly between the values for pure Si and pure Ge [20]. The electronic Hamiltonian of the system is represented by an $sp^3d^5s^*$ nearest-neighbour tight-binding model. We have adopted the semi-empirical parameters of bulk pure Si and Ge and their scaling laws reported in [17]. Once the interatomic distances and the strain tensor in the alloy lattice are known, the geometrical phase factors of the tight-binding Hamiltonian are modified according to the new interatomic distances while site energies and Slater–Köster hopping interactions are scaled as given in [17]. The virtual-crystal approximation is adopted to obtain the alloy parameters, with linear interpolation of self-energies and two-centre integrals. This procedure uniquely defines the tight-binding first-neighbour Hamiltonian of the substrate and of the active material. We have first studied the electronic band structure of the isolated infinite crystal alloy $Si_{1-x}Ge_x$ under the same strain conditions it suffers when epitaxially grown on a (001)-$Si_{1-y}Ge_y$ substrate, i.e. with $a_\parallel(x) = a_0(y)$ and $a_\perp(x)$ given by expression (2). The results are reported in figures 1(a)–(d). Figure 1(a) shows the fundamental energy gap of the active material as a function of x and y. The line $x = 0$ represents the case of pure strained Si grown on an alloy with Ge fraction y; the line $y = 0$ reproduces the gap of a strained alloy with x Ge fraction, grown on pure Si and

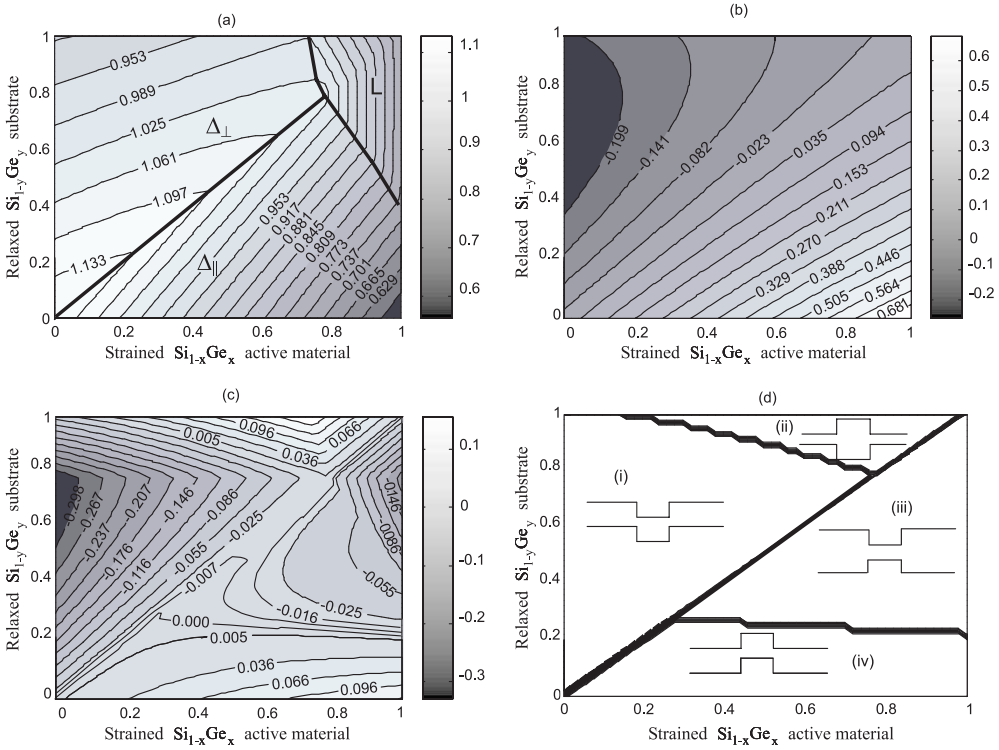

Figure 1. (a) Fundamental bandgap energies; (b) valence band offsets; (c) conduction band offsets and (d) band-edge profiles of $Si_{1-x}Ge_x$ alloy as a function of the Ge concentration in the strained active material (x axis) and y Ge concentration in the alloy substrate (y axis) which determines the $a_\parallel$ lattice constant of the active layer (see text). Energies are in electronvolts.

so on. Our calculations qualitatively confirm the results of [9]: the biaxial distortion breaks the sixfold degeneracy of the Δ line in $\vec{k}$-space giving rise to a twofold degenerate $\Delta_\perp$ axis and a fourfold degenerate $\Delta_\parallel$ axis. We can therefore distinguish in figure 1(a) three domains according to the point in the $\vec{k}$ space which realizes the bottom of the conduction band: a first region, for $x < y$, where the bottom is along the orthogonal axis $\Delta_\perp$, a second region for $x > y$ where it is along the parallel direction $\Delta_\parallel$, and a third one characterized by weakly strained alloys with high Ge content where the bottom of the conduction band occurs at the L point and then the alloy is Ge-like. The gap assumes its largest value for the case of relaxed Si ($x = 0$, $y = 0$), and the smallest value for strained pure Ge grown on pure Si ($x = 1$, $y = 0$). In the literature some authors (see for instance [9, 3]) find that the fundamental energy gap of strained Ge grown on Si is larger than that of strained Si grown on Ge substrate while others [21, 22] support the opposite. The first step for the evaluation of the band lineups at the heterointerface is the knowledge of the valence band offset (VBO) between strained $Si_{1-x}Ge_x$ active layer and the relaxed $Si_{1-y}Ge_y$ substrate. Figure 1(b) reports the results obtained exploiting the valence band offsets calculated for pure Si/Ge interfaces in the whole range of strain conditions [23] and interpolating linearly between the Si/Ge value and zero, which occurs for the interface between relaxed $Si_{1-y}Ge_y$ and strained $Si_{1-x}Ge_x$ with $x = y$; eventually we obtain

$$\mathrm{VBO}(x, y) = (x - y)\,(0.74 - 0.53y)\ \mathrm{eV}. \tag{3}$$

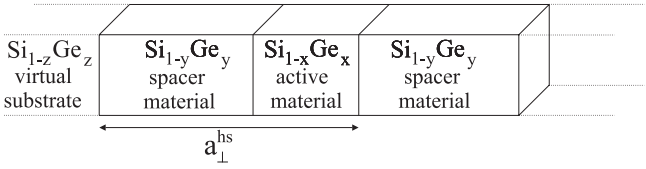

Figure 2. Schematic representation of the (001)-grown Si/Ge heterostructure described in the text.

We just want to stress that VBO(x, y) is greater than zero for $x > y$ and reaches the maximum value of 0.74 eV for fully strained germanium on Si ($x = 1, y = 0$). From the knowledge of the fundamental bandgap and of the valence band offsets, we can evaluate the conduction band offset (CBO), which is defined as the difference between the lowest conduction band energy in the active layer and in the substrate. Thus a negative (positive) CBO means type-I (II) band alignment. Figure 1(c) summarizes our result. As in [9] we find positive CBOs for all x if the substrate is poor in Ge concentration. We confirm that negative CBO, up to -0.3 eV, characterizes the region with $x < 0.3$ and $0.4 < y < 0.8$. It is worth mentioning that our numerical values for this region are smaller in modulus than those reported in [9], and are closer to the results obtained in the same (x, y) region by Schäffler [3] by means of deformation potential theory and by Paul [2], who reports values obtained scaling those of [9] to fit experimental evidence. Moreover, the values of the CBOs in the upper-right corner of figure 1(c) below the diagonal are also negative, as in [9, 3], although larger in magnitude: for example, for $x = 1$ and $y = 0.8$ we have CBO $= -0.224$ to be compared with the value CBO $\simeq -0.1$ eV reported in [9]. Finally, a novelty of our results is the presence of a (x, y) region defined by $0.4 < x < 1$ and $0.8 < y < 1$, evidenced in figure 1(c) by an upside triangular shape, which is characterized by positive CBOs up to the value 0.187 eV for $x = 0.74$ and $y = 1$. This region is absent in [9] where the active material with $x < y$ always presents a negative CBO but it is predicted in [3, 24]. Before concluding this paragraph we summarize our result for band alignment as shown in figure 1(d); in the (x, y) space we distinguish four regions according to the sign of VBO and CBO produced at the interface. In region (i) VBO < 0 and CBO < 0, in region (ii) VBO < 0 and CBO > 0, in region (iii) VBO > 0 and CBO < 0 and finally in region (iv) VBO > 0 and CBO > 0. As is well known, a type-I alignment for band edges, that we predict for region (iii), is well suited for opto-electronic application: embracing a slice of active layer from both sides with cubic $Si_{1-y}Ge_y$ alloys and choosing (x, y) in region (iii), we obtain a device with both types of carriers at the fundamental gap spatially confined in the active layer zone. In the next paragraph we further investigate this region with an analysis of the $\vec{k}$-space structure of the energy bands.

3. Direct gap—type-I Si/Ge heterostructures

From the information on band alignment presented in the previous section we investigate now the possibility of realization of a type-I heterostructure with fundamental gap occurring between states at the same $\vec{k}$-point. Allowed direct transitions both in $\vec{r}$- and in $\vec{k}$-space should significantly increase the efficiency of charge recombination in the device. Occurrence of a direct gap and confinement of holes and electrons in the active material region can be demonstrated only by diagonalizing the Hamiltonian operator that describes the whole structure made by buffer, spacer material and active material (see figure 2). This operator is constructed following the approach outlined in the previous section for the case of

bulk materials and accounts for strain and spin–orbit effects as already discussed. The VBO between regions of the system with different Ge content is inserted as an additional contribution to the diagonal matrix elements of the system Hamiltonian. The general heterostructures we have analysed can be described as follows (see figure 2): n_a layers of *active* $Si_{1-x}Ge_x$ material with Ge concentration x are embedded between two thick spacer regions of $Si_{1-y}Ge_y$ alloys with Ge concentration y. Each spacer region consists of n_s layers. The lattice constant in the plane parallel to the interface is determined by a virtual relaxed $Si_{1-z}Ge_z$ substrate. The interlayer separations in the active and in the spacer regions are given by $a_\perp(x)/4$ and $a_\perp(y)/4$, respectively. These lengths are evaluated by equation (2), where the $a_\parallel$ value is determined by the Ge concentration in the substrate. In this way we have the possibility to tune independently both the strain conditions (varying the z concentration parameter and thus $a_\parallel$) and the valence band offset between the spacer and the active region (varying the y concentration parameter). Note that both the spacer and the active alloys are tetragonally distorted. If the spacer regions are thick enough the region of the active material can be considered as an isolated quantum well. Periodic boundary conditions are imposed on the supercell with $a_\perp^{hs}$ orthogonal extension along the (001) direction. In our simulations we have chosen $n_a + n_s = 800$ and n_a varying from 4 up to 100. As a consequence, the primitive cell contains 800 atoms. Thus the evaluation of band structure at a generic $\vec{k}$-point requires the diagonalization of a matrix of order $2 \times 10 \times 800$, 800 being the total number of layers in the primitive cell and 2×10 (ten orbitals and two spin states) the number of basis functions localized on each layer. The tight-binding renormalization method is particularly efficient in treating such long period superlattices. We have presented elsewhere the details of this method, thus we summarize here only a few steps of the procedure. The Hamiltonian of the whole system is first represented on the basis of two-dimensional Bloch sums built from layer orbitals [25, 26]. Then an iterative decimation–renormalization procedure is performed [27] to reduce the cell to a couple of interacting effective layers where the Green's function can be evaluated. At each step of the iteration only inversion of small (20×20) matrices is required. From the Green's function the spectral properties of the system are obtained without explicit diagonalization of the Hamiltonian; in particular layer and orbital resolved electron and hole densities can be deduced. The basis vectors of the (tetragonal) primitive cell of the device are $\vec{w}_1 = \frac{a_\parallel}{2}(110)$, $\vec{w}_2 = \frac{a_\parallel}{2}(110)$ and $\vec{w}_3 = a_\perp^{hs}(001)$; $a_\parallel$ is given by the matching condition with the relaxed $Si_{1-z}Ge_z$ substrate, $a_\perp^{hs}$ measures the extension of the cell in the growth direction (see figure 2) and is obtained by multiplying the number of layers of each region by their mutual separation deduced from equation (2), and then summing the contributions from the two strained regions. Due to the large periodicity of the system along the growth direction the first Brillouin zone has vanishing thickness in the same direction. This implies that folding effects are expected for the states along the (001) line. Just to make an example, if we describe a bulk Si crystal as a long period multilayer made of a very large number of Si planes, the eigenvalues corresponding to the L point at $\frac{2\pi}{a_\parallel}(\frac{1}{2}\frac{1}{2}\frac{1}{2})$ fold into the two dimensional Brillouin zone at the L′ point with coordinates $\frac{2\pi}{a_\parallel}(\frac{1}{2}\frac{1}{2}0)$. Similarly, the $\Delta_\perp$ line folds into the Γ point but the $\Delta_\parallel$ lines remain unaltered: this folding mechanism is more complex for short period superlattices [28, 29] and is crucial to obtain a direct gap device. Guided by the information obtained from figure 1(d) we have focused on the multilayer structure shown in figure 2, with parameters $x = 1$, $y = 0.75$ and with $a_\parallel$ determined by a substrate alloy with $z = 0.8$. In fact, if we preliminarily neglect the (small) strain conditions present in the spacer material, the chosen (x, y) concentration values belong to region (iii) of figure 1(d), thus providing a type-I heterointerface. Before presenting the results obtained from the full diagonalization of this heterostructure, we formulate the same preliminary analyses based on folding considerations

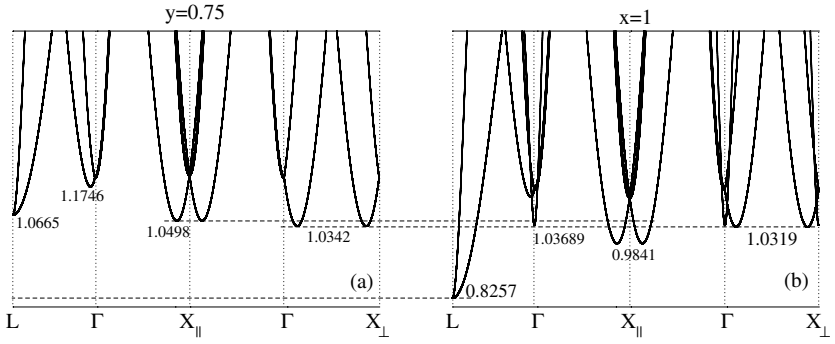

Figure 3. Conduction band profiles of the isolated spacer region alloy (a) and of the isolated active region (b) alloy with Ge concentration $y = 0.75$ and $x = 1$, respectively. $a_\parallel$ is matched with the lattice constant of the substrate alloy whose Ge concentration is $z = 0.8$. The zero of energy is fixed at the top of the valence band of the spacer material. Dashed lines are a reference for the eye and energies are in electronvolts.

and band edge profiles of the isolated alloy $Si_{0.25}Ge_{0.75}$ and of the isolated pure Ge crystal, both tetragonally deformed to account for the $a_\parallel$ lattice constant required by matching with a relaxed substrate alloy $Si_{0.2}Ge_{0.8}$. The VBO in the Ge active material region amounts to 0.079 eV, thus it acts as a well for the holes at the top of the valence band, at the Γ point. The VBO between the y and x regions is evaluated using the top of the valence band in the substrate as reference energy; in the plots shown in the following we use as zero energy of the complete structure the top of the valence band in the y region. The results for the conduction band structures are reported in figure 3(a) for the spacer material and in figure 3(b) for the active material, respectively. From figures 3(a) and (b) it is evident that the minimum of the conduction bands is at the L point in the active material and that $E_L(x) < E_L(y)$. Therefore, we argue that when we pass to the corresponding multilayer structure of figure 2, at the folded L′ point ($\vec{k} = \frac{2\pi}{a_\parallel}(\frac{1}{2}\frac{1}{2}0)$) the potential experienced by the conduction electrons produces states confined in the active region material. The same situation is expected for the minimum along the $\Delta_\parallel$ lines which occurs for both alloys at about 0.85 of the Γ–$X_\parallel$ separation, no folding effect being in fact expected for the $\Delta_\parallel$ lines. As concerns the $\vec{k}$ points along the $\Delta_\perp$ line we see from figure 3(a) that in the spacer (y) material the minimum along the $\Delta_\perp$ line is lower in energy than the minimum along the $\Delta_\parallel$ line (see also figure 1(a) for the region of biaxial tensile strain). As already noticed, this energy separation is due to the biaxial strain deformation induced by the z cubic substrate. Furthermore, the energy of the minimum along $\Delta_\perp$ in the active material is slightly lower in energy than in the spacer material. This means that another well for electrons is expected along $\Delta_\perp$; the confined states in this well are folded at Γ and are lower in energy than the unfolded states at Γ. The scheme of figure 4 summarizes the potential profile for the conduction electrons of the complete multilayer that we predict for $\vec{k}$-points at L′, Γ and along $\Delta_\parallel$ (the states along $\Delta_\perp$ are folded in Γ). It is appropriate to remark once more that strain in the spacer material is essential to make the edges of the well at Γ lower than those at $\Delta_\parallel$. This makes evident the need of a third alloy acting as cubic substrate. It is interesting to examine the crucial role played by confinement induced by the active material thickness. Suppose first that the active Ge region consists of a large number of layers. Then the well width for the conduction electrons is large and the lowest confined states lie near to the bottom of each well (figure 4, solid lines). As a consequence, the lowest conduction state occurs at L′ and its energy tends to the limit value of 0.8257 eV, which is the lowest energy value of conduction electrons in the strained active region at L; see figure 3(b).

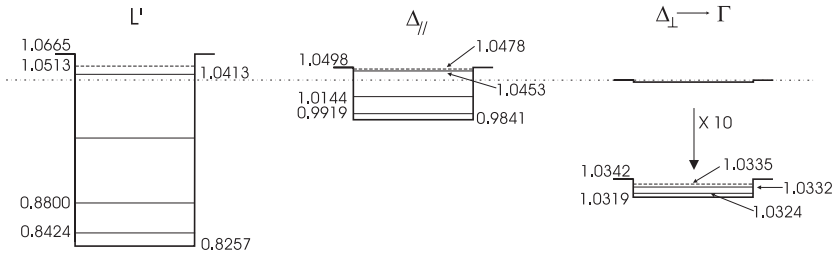

Figure 4. Schematic view of the well energy profiles at L′, $\Delta_\parallel$ and Γ experienced by electrons at the bottom of the conduction band of the $Si_{0.25}Ge_{0.75}$/Ge structure defined in the text. The energy levels for the confined states are reported with solid lines for the case $n_a = 80$ and with dashed lines for $n_a = 4$. The dotted–dashed line is a reference for the eye. The reference of energy is at the top of the valence band in the spacer material.

The fundamental gap is thus indirect in $\vec{k}$-space; in fact the topmost of the valence bands of the complete structure is always at the Γ point. If we now choose an active region composed by few layers the lowest confined states at L′, $\Delta_\parallel$ and Γ rise in energy approaching the edges of each well (see figure 4, dashed lines). Therefore, due to the fact that $E_{\Delta_\parallel}(y) > E_{\Delta_\perp}(y)$, in the limit of thin active region, the lowest (confined) state lies at Γ. This means that a transition from $\vec{k}$-indirect to $\vec{k}$-direct gap material should be observed as the number of layers of the active region decreases. Figure 5 demonstrates that a full band structure calculation obtained by the decimation–renormalization procedure confirms our conjectures. Figures 5(a) and (c) correspond to the active region made by $n_a = 4$ and $n_a = 80$ monolayers, respectively. As a check calculation, we have also evaluated the electronic structure for the case $n_a = 0$, i.e. considering only the 800 monolayer thick $Si_{0.25}Ge_{0.75}$ strained alloy. The results reported in figure 5(b) are thus the Γ-folded picture of the band structure shown in figure 3(a). The total number of layers for the structures described in the figures 5(a)–(c), is $n_s + n_a$ and is kept constant and equal to 800. In the case of large ($n_a = 80$) well width, four (two) confined bands at L′ ($\Delta_\parallel$) are clearly visible if figure 5(c). In the few monolayer regime ($n_a = 4$) the wells confine only one level (see also figure 4), which is close to the edge of the wells and hence near in energy to the continuum of states visible in figure 5(a) at the L′ point (the confined state at $\Delta_\parallel$ is too close to the continuum levels to be visible on this energy scale). These subbands lie above the bottom of the conduction level, which is at the Γ point. The inset of figure 5(b) shows a detail of the conduction energy bands around the Γ point for the structure of figures 5(a) and (b). The presence of a confined state at Γ is evident and this realizes a genuine fundamental direct gap both in real and in $\vec{k}$-space. The numerical values of the eigenvalues with energy below the edges of the wells at L′, Γ and $\Delta_\parallel$ are reported in figure 4. To check the spatial confinement of these states, we have calculated for each of them the density of states projected on the layers of the structure. Some of them are reported in figure 6. We notice that although the best confinement effect occurs for the deepest well at L′, a few millielectronvolts of well depth at Γ are enough to produce confinement. We have checked that also the topmost valence state, which occurs at Γ, is confined in the active material region, and this confirms the possibility of a direct-gap type-I transition in the device. This fundamental transition is dipole allowed as we have verified, analysing the angular momentum character of the states involved in the transition.

Eventually we have evaluated the dipole matrix elements along $\hat{x}$, $\hat{y}$ and $\hat{z}$ directions for the direct fundamental transition ($n_a = 4$), which is the key information for an optically useful device. In our tight-binding scheme only the self-energies and hopping parameters of the Hamiltonian are used and no explicit knowledge of the localized basis set $\{\psi_i\}$ is

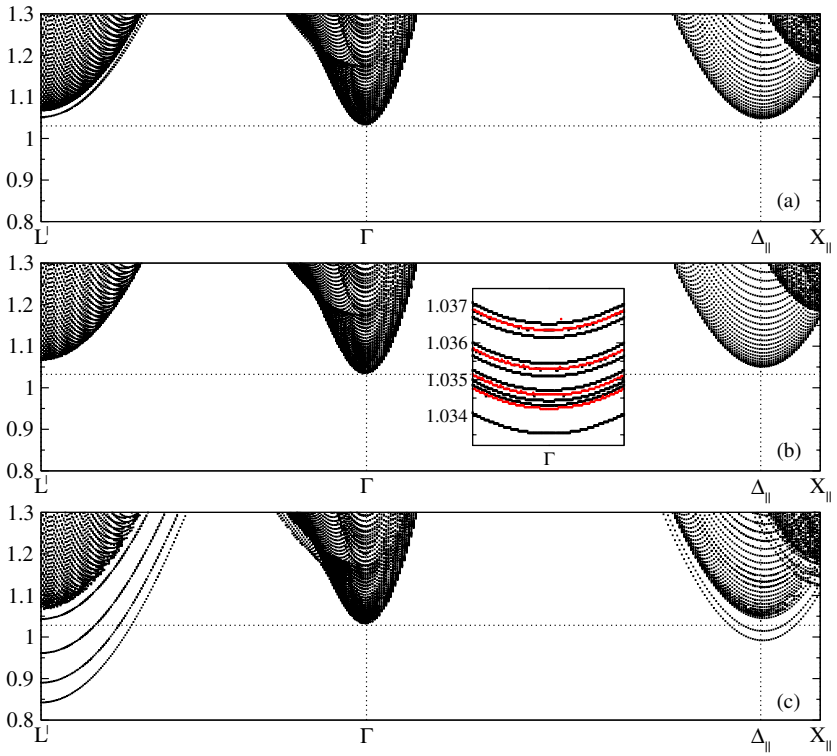

Figure 5. Conduction band structures of the system represented in figure 2 with $n_a = 4$ (a), $n_a = 0$ (b) and $n_a = 80$ (c) monolayers in the active Ge region. $n_s + n_a$ is kept constant and equal to 800. The inset shows a detail of the band structure around the Γ point of (a) (black bands) superimposed on the band structure corresponding to the case $n = 0$ (grey bands).

(This figure is in colour only in the electronic version)

required. As a consequence, after diagonalization of the matrix Hamiltonian, the $\vec{p}$ matrix elements between the states involved in the transitions are obtained from the relation [30, 31] $\langle\psi_i|\vec{p}|\psi_j\rangle \simeq \mathrm{im}\langle\psi_i|H|\psi_j\rangle\vec{d}_{ij}/\hbar$, where $\vec{d}_{ij}$ is the vector connecting the orbitals in sites i and j. Before applying this scheme of calculus to the system of interest, we have checked its reliability, verifying that the dipole selection rules for $\hat{x}$, $\hat{y}$ and $\hat{z}$ polarization, derived in the paper of [21] in the case of biaxially strained bulk materials, are respected. Furthermore, we have verified that states of bulk materials which fold at the Γ point when an artificial long period multilayer description is adopted (as is the case of figure 5(b)) have zero dipole matrix element with the Γ topmost valence state, as one can expect due to the fact that these states do not belong to Γ representations. On the other hand, this is not the case for the direct gap heterostructure under investigation due to the presence of interfaces and confinement effects. Indeed, we have found that the fundamental direct transition at Γ is dipole allowed for $\hat{z}$-polarization, but the value of the matrix element is two orders of magnitude smaller than the optical transition $\Gamma_8^+ \rightarrow \Gamma_6^-$ in bulk Ge under the same strain conditions.

4. Conclusions

We have adopted an $sp^3d^5s^*$ first neighbour tight binding Hamiltonian with spin–orbit coupling to evaluate the electronic properties of strained $Si_{1-x}Ge_x$ alloy grown on $Si_{1-y}Ge_y$

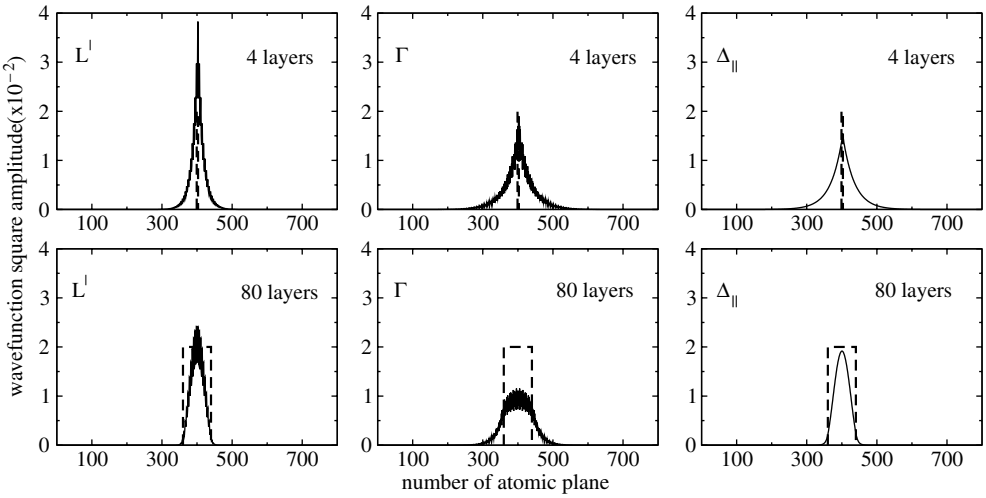

Figure 6. Localization properties of the wavefunction square amplitude for the lowest conduction states at L′, Γ and $\Delta_{\|}$ in the case of active Ge material made by $n_a = 4$ monolayers (upper row) and for $n_a = 80$ (lower row). The plots represent the integration of the density of states in a small energy region around the eigenvalue of the state. The dashed lines indicate the Ge well region. The topmost valence state is located in the same Ge region.

relaxed substrate along the (001) direction. The strain effects are treated by means of a set of scaling laws for the hopping energies of the biaxially distorted lattice together with exact calculation of the geometrical phase factors. Linear interpolation with respect to Ge concentration is used both to define the alloy tight-binding parameters and the valence band offsets. We have obtained the fundamental energy gap for the strained alloy and the conduction and valence band offsets at the heterointerface in the whole range of Ge concentrations, both in the strained material and in the substrate. Some of our results are in qualitative agreement with the results of Rieger and Vogl [9] obtained from the empirical pseudopotential method. In particular, we confirm a small positive CBO for the strained $Si_{1-x}Ge_x$ alloy with $0 < x < 1$ grown on Si substrate. Furthermore, as for the authors of [9], robust type-I alignment for Ge-rich strained alloys on Ge-rich substrate is obtained. Anyway, we observe a region centred around $x \simeq 0.7$ and $y \simeq 1$ in the (x, y) plane which is absent in [9]. This region is characterized by negative VBO and positive CBO and is also predicted in the review article by Schäffler [3]. To our knowledge, no experimental evidence exists to characterize spatial confinement of charges in the conduction band of multilayer structures with high Ge concentration both in the active region and in the substrate. Indeed, the interest in such heterostructures has recently grown, mainly motivated by the study of valence intersubband transitions [32].

With the purpose of obtaining a type-I and direct fundamental gap device, in the second part of this work we investigated a family of multilayer Si/Ge heterostructures composed by a region of active material embedded in a spacer alloy. The lattice constant of the multilayer has been determined by the presence of a third material acting as virtual substrate: this has allowed us to vary strain conditions independently from band lineups at the heterointerfaces. Proper alloy conditions in the substrate, spacer and active regions which lead to type-I and direct gap devices have been found. The case of pure Ge between $Si_{0.25}Ge_{0.75}$ alloy grown on a $Si_{0.2}Ge_{0.8}$ substrate has been chosen to present a type-I direct gap heterostructure. The $\vec{k}$-direct fundamental transition localized in the Ge region is indeed dipole allowed as

confirmed by optical matrix element analysis but remains two orders of magnitude smaller than a typical direct transition in bulk germanium. We have verified that once the direct gap conditions are realized for the four-monolayer germanium well with the chosen values of x and z concentrations the direct nature of the fundamental transition is preserved, provided the width of the spacer guarantees the folding of the $\Delta_\perp$ minima into the Γ point. This enriches the flexibility of the proposed geometry for practical realizations.

Acknowledgment

This work has been supported by the National Enterprise for NanoScience and NanoTechnology (NEST).

References

[1] Yang L, Watling J R, Wilkins R C W, Boriçi M, Barker J R, Asenov A and Roy S 2004 *Semicond. Sci. Technol.* **19** 1174
[2] Paul D J 2004 *Semicond. Sci. Technol.* **19** R75
[3] Schäffler F 1997 *Semicond. Sci. Technol.* **12** 1515
[4] Jain S C, Willis J R and Bullough R 1990 *Adv. Phys.* **39** 127
[5] Braunstein R, Moore A R and Herman F 1958 *Phys. Rev.* **109** 695
[6] Bublik V T, Gorelik S S, Zaitsev A A and Polyakov A Y 1974 *Phys. Status Solidi* **65** K79
[7] People R and Bean J C 1986 *Appl. Phys. Lett.* **48** 538
[8] Van de Walle C G and Martin R M 1986 *Phys. Rev.* B **34** 5621
[9] Rieger M M and Vogl P 1993 *Phys. Rev.* B **48** 14276
[10] Penn C, Schäffler F, Bauer G and Glutsch S 1999 *Phys. Rev.* B **59** 13314
[11] Wachter M, Thonke K, Sauer R, Schäffler F, Herzog H J and Kasper E 1992 *Thin Solid Films* **222** 10
[12] Baier T, Mantz U, Thonke K, Sauer R, Schäffler F and Herzog H J 1994 *Phys. Rev.* B **50** 15191
[13] Fukatsu S and Shiraki Y 1993 *Appl. Phys. Lett.* **63** 2378
[14] Northrop G A, Morar J F, Wolford D J and Bradley J A 1992 *J. Vac. Sci. Technol.* B **10** 2018
[15] Houghton D C, Aers G C, Eric Yang S R, Wang E and Rowell N L 1995 *Phys. Rev. Lett.* **75** 866
[16] Thewalt M L W, Harrison D A, Reinhart C F, Wolk J A and Lafontaine H 1997 *Phys. Rev. Lett.* **79** 269
[17] Jancu J M, Scholz R, Beltram F and Bassani F 1998 *Phys. Rev.* B **57** 6493
[18] Virgilio M, Farchioni R and Grosso G 2005 *Phys. Rev.* B **71** 155302
[19] Dismukes J P, Ekstrom L and Paff R J 1964 *J. Phys. Chem.* **68** 3021
[20] Madelung O (ed) 1989 *Landolt-Börnstein New Series* Group III vol 17a (Berlin: Springer)
[21] Ma Q M, Wang K L and Schulman J N 1993 *Phys. Rev.* B **47** 1936
[22] Fischietti M V and Laux S E 1996 *J. Appl. Phys.* **80** 2234
[23] Colombo L, Resta R and Baroni S 1991 *Phys. Rev.* B **44** 5572
[24] Davies J H 1998 *The Physics of Low-Dimensional Semiconductors* (Cambridge: University Press) p 101
[25] Grosso G, Moroni S and Pastori Parravicini G 1989 *Phys. Rev.* B **40** 12328
[26] Grosso G, Pastori Parravicini G and Piermarocchi C 1996 *Phys. Rev.* B **54** 16393
[27] Grosso G and Pastori Parravicini G 2000 *Solid State Physics* (London: Academic)
[28] Satpathy S, Martin R M and Van de Walle C G 1988 *Phys. Rev.* B **38** 13237
[29] Schmid U, Christensen N E, Alouani M and Cardona M 1991 *Phys. Rev.* B **43** 14597
[30] Ren S Y and Harrison W A 1981 *Phys. Rev.* B **23** 762
[31] Brey L and Tejedor C 1983 *Solid State Commun.* **48** 403
[32] see e.g. Fromherz T, Meduňa M and Bauer G 2005 *J. Appl. Phys.* **98** 44501 and references therein